Inorganic Chemistry

Article

pubs.acs.org/IC

Calcium Phosphonate Frameworks for Treating Bone Tissue Disorders

Fa-Nian Shi,[†,‡] José C. Almeida,[§] Luisa A. Helguero,[∥,⊥] Maria H. V. Fernandes,[§] Jonathan C. Knowles,[#] and João Rocha*[,‡]

[†]School of Science, Shenyang University of Technology, 110870 Shenyang, China

[‡]Department of Chemistry, and [§]Department of Materials and Ceramic Engineering, CICECO-Aveiro Institute of Materials, University of Aveiro, 3810-193 Aveiro, Portugal

[∥]Organic Chemistry and Natural Products Unit (QOPNA), Department of Chemistry, University of Aveiro, 3810-193 Aveiro, Portugal

[⊥]Institute for Research in Biomedicine−iBiMED, Health Sciences Program, University of Aveiro, 3810-193 Aveiro, Portugal

[#]Division of Biomaterials and Tissue Engineering, UCL Eastman Dental Institute, University College London, London, WC1X 8LD, United Kingdom

Supporting Information

ABSTRACT: Two new examples of uncommon three-dimensional Ca-bearing metal organic frameworks, $[Ca(H_2O)_3(HPXBP)]$ (**CaP1**) and $[Ca_2(H_2O)_2(HPXBP)_{1.5}]$ (**CaP2**) (PXBP: *p*-xylylenebisphosphonate), were prepared and their structures characterized by single crystal X-ray diffraction. **CaP1** crystallizes in the monoclinic $C2/c$ space group, with three water molecules occupying a half coordination sphere on one side of the Ca atom, while **CaP2** crystallizes in the triclinic $P\bar{1}$ space group, with two crystallographic unique Ca atoms, each coordinated by a single water molecule. In contrast with **CaP2**, which exhibits very low bioactivity, **CaP1** readily precipitates bone-precursor phases (octacalcium phosphate, OCP, and hydroxyapatite) in SBF solutions. Moreover, studies with MG63 osteoblast-like cells indicate that **CaP1** is not toxic and stimulates bone mineralization and, thus, holds considerable potential for treating bone diseases, such as osteoporosis.

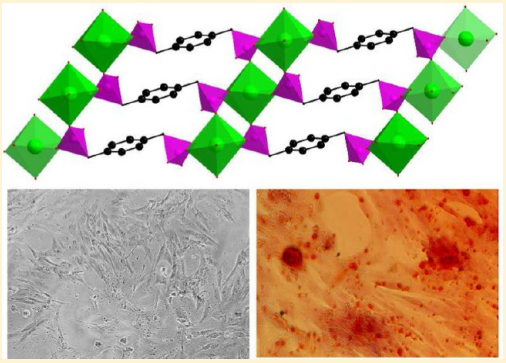

INTRODUCTION

Calcium is a key component of, among others, bones and teeth, accounting for about 2% of human body weight.[1] Because calcium is not produced in the body, but is present in milk and other dairy products, it must be taken in as part of a healthy diet.[2−4] Although calcium carbonate is a common low-cost calcium supplement, it is also poorly digested and absorbed due to its low solubility in bodily fluids.[5] Caltrate is a popular commercial calcium supplementation solution whose main components are calcium carbonate and Vitamin D3. However, taken in excess, vitamin D3 may be harmful.[6] Therefore, there is much scope for introducing new bioactive calcium chemicals.

Bisphosphonates are primary agents in the current pharmacological arsenal against osteoclast-mediated bone loss due to osteoporosis, Paget's disease of bone, metastasis to the bone, and malignancy-associated hypercalcemia.[7,8] Bisphosphonates were introduced to clinical practice some four decades ago, and they are important when an imbalance between osteoblast-mediated bone formation and osteoclast-mediated bone resorption underlies disease pathology. Indeed, bisphosphonates have the ability to inhibit calcification and hydroxyapatite breakdown, thereby effectively suppressing bone resorption. All bisphosphonates present very high affinity for (and consequent deposition into) bone relative to other tissues, allowing them to achieve a high local concentration throughout the entire skeleton. Despite the benefits of bisphosphonates, the recent recognition that their use is associated with pathologic conditions including the osteonecrosis of the jaw prompts research into new types of related materials.

Although the maintenance of adequate calcium (and vitamin D) intake is crucial for all patients receiving bisphosphonate therapy, this is frequently overlooked. We have, thus, reasoned that it is of interest to use bioactive materials comprising Ca^{2+} and a bisphosphonate molecule, rather than supplying calcium and bisphosphonate separately. A search on the online CSD database[9] revealed 74 different Ca-phosphonates structures and work mainly focused on structural description and physical properties;[10−14] only two examples of potential biomaterials are available.[15,16] As a first step exploring this concept, here we report two new Metal Organic Frameworks formulated as $[Ca(H_2O)_3(HPXBP)]$ (**CaP1**) and $[Ca_2(H_2O)_2(HPXBP)_{1.5}]$

Received: July 28, 2015
Published: September 25, 2015

DOI: 10.1021/acs.inorgchem.5b01634
Inorg. Chem. 2015, 54, 9929−9935

(**CaP2**), where PXBP depicts *p*-xylylenebisphosphonate. **CaP1** readily precipitates bone-precursor phases in simulated body fluid (SBF), while studies with MG63 osteoblast-like cells indicate that it is not toxic and promotes bone mineralization.

EXPERIMENTAL SECTION

The following reagents were readily available from commercial sources and were used as received without further purification: calcium chloride dihydrates ($CaCl_2{\cdot}2(H_2O)$, 99.0+%, Alfa Aesar), calcium hydroxide ($Ca(OH)_2$, ≥95.0%, Alfa Aesar), and tetraethyl-*p*-xylylenebisphosphonate (TEPP, $C_{16}H_{28}O_6P_2$, ≥98%, Epsilon Chimie). The final products were air- and light-stable, and insoluble in water.

Synthesis of Single Crystals of $[Ca(H_2O)_3(C_8H_{10}O_6P_2)]$ (CaP1). A mixture of 0.1374 g of $CaCl_2{\cdot}2(H_2O)$ (0.93 mmol) and 0.1094 g of $C_{16}H_{28}O_6P_2$ (0.29 mmol) in ca. 10 g of distilled water was stirred thoroughly in air for half an hour yielding a transparent colorless solution, which was placed into a 25 mL autoclave and in preheated oven, at 180 °C. After 3 days the autoclave was cooled to room temperature and the liquor within (pH = 2) was carefully moved into a clean glass container (25 mL) by filtration, and the excess water was allowed to slowly evaporate. After 1 day, large block colorless single crystals of **CaP1** were harvested from the bottom and the round wall of the glass container. The particles were carefully collected manually, washed with distilled water, and air-dried at ambient temperature. The yield was ca. 0.05 g, and 48% based on the ligand. The phase purity was confirmed by powder XRD (Figure S1). Calculated elemental composition (based on single-crystal data; in %): C 26.80, H 4.47. Found (%): C 26.20, H 4.52.

Synthesis of Single Crystals of $[Ca_2(H_2O)_2(C_8H_{9.3}O_6P_2)_{1.5}]$ (CaP2). A mixture of 0.1616 g of $CaCl_2{\cdot}2H_2O$ (1.10 mmol), 0.0740 g of $Ca(OH)_2$ (1.06 mmol), and 0.2014 g of $C_{16}H_{28}O_6P_2$ (0.53 mmol) in 10 g of distilled water was stirred thoroughly in air for half an hour yielding a white turbid solution. The solution was moved into a 25 mL autoclave and put into a preheated oven at 180 °C. After 3 days it was cooled down to room temperature, the mother liquor (pH > 3) was filtered away, and white plate-like particles washed with copious amounts of distilled water (3 × 10 mL) and dried at room temperature to give pure **CaP2** (ca. 0.25 g yield and 61% based on the ligand) as revealed by powder XRD (Figure S2). Calculated elemental composition (based on single-crystal data; in %): C 28.16, H 3.52. Found (%): C 27.89, H 3.64.

General Characterization. C and H elemental analyses were performed using a TruSpec 630−200−200 elemental analyzer with a combustion furnace temperature of 1075 °C and an after-burner temperature of 850 °C. SEM (scanning electron microscopy) and EDX (energy dispersive X-ray spectroscopy) were performed on a Hitachi SU-70 microscope equipped with a Bruker QUANTAX 400 X-ray microprobe. The particles or pellets were fixed with conductive carbon gel and coated with carbon. Powder X-ray diffraction patterns (PXRD) were recorded at room temperature using an Empyrean diffractometer with Cu Kα radiation (1.54178 Å) in the 2θ range of 5−50° in transmission mode at 45 kV and 40 mA.

FT-IR spectra of **CaP1** and **CaP2** were collected from KBr pellets (Aldrich 99%+, FT-IR grade) on a Mattson 7000 FT-IR spectrometer. The main CaP1 bands (cm^{-1}) are 3592(s), 3480(s), 3395(s), 3026(w), 2907(m), 2775(m), 2473(m), 2340(m), 2228(m), 1669(s), 1517(m), 1412(w), 1306(s), 1253(s), 1161(s), 1128(s), 1062(s), 1016(s), 937(s), 844(m), 720(m), 621(m), 561(s), 482(s), 442(s). The main CaP2 bands (cm^{-1}) are 3500(s), 3342(s), 3224(s), 3020(w), 2907(m), 2775(m), 2492(w), 2406(w), 2361(m), 1662(m), 1622(m), 1510(m), 1412(w), 1259(s), 1167(s), 1115(s), 1035(s), 976(s), 911(s), 831(m), 720(w), 646(w), 568(s), 489(s), 449(s).

Thermogravimetric analyses (TGA) were carried out using a Shimadzu TGA 50, with a heating rate of 5 °C/min under air. Weight losses for **CaP1**: 40−108 °C, 4.6%; 108−150 °C, 5.5%; 150−215 °C, 4.4%; 215−460 °C, 4.7%; 520−770 °C, 25.3% (weight loss balance). Weight losses of **CaP2**: 20−242 °C, 3.4%; 242−280 °C, 4.0%; 280−468 °C, 4.1%; 468−770 °C, 23.7% (weight loss balance).

X-ray Crystallography. Complete single-crystal data of **CaP1** and **CaP2** were collected at 180(2) K on a Bruker X8 Kappa APEX II charge-coupled device (CCD) area-detector diffractometer (Mo Kα graphite monochromated radiation, λ = 0.7107 Å) controlled by the APEX2 software package and equipped with an Oxford Cryosystems Series 700 cryostream monitored remotely by using the software interface Cryopad. Images were processed using the software package SAINT+. Absorption corrections were applied by the multiscan semiempirical method implemented in SADABS. The structure was solved by direct methods using SHELXS-97[17] and refined with SHELXL-97.[18] All non-hydrogen atoms were successfully refined with anisotropic displacement parameters. Hydrogen atoms bound to carbon were located at their idealized positions by employing the HFIX 43 and HFIX 23 instructions in SHELXL-97 and included in subsequent refinement cycles in riding motion approximation with isotropic thermal displacement parameters (Uiso) fixed at 1.2 Ueq of the carbon atom to which they were attached. Hydrogen atoms of water molecules were located from difference Fourier maps and isotropically refined with the O−H and H···H distances restrained to 0.85(1) and 1.45(2) Å, respectively, and Uiso values were set equal to 1.2 Ueq (parent atom) for water H atoms. PLATON was used for the cif files check.[19] The detailed crystallographic data and structural refinement parameters are summarized in Table S1. Selected bond lengths and angles are given in Table S2 and hydrogen bonding parameters are listed in Table S3. Complete crystallographic data were deposited in CIF format with the Cambridge Crystallographic Data Center as supplementary publication numbers of CCDC 1050980 and CCDC 1050981. Copies of the data can be obtained free of charge on application to CCDC, 12 Union Road, Cambridge CB2 1EZ, UK (fax: (44) 1223336−033; e-mail: deposit@ccdc.cam.ac.uk).

Soaking Tests in Simulated Body Fluid. Surface modification was evaluated *in vitro* by immersion of pressed pellets of the produced materials in Kokubo's[20] simulated body fluid (SBF) for 3, 7, 9, 12, and 14 days. After soaking, the samples were dried under 60 °C in air, and then the surface of the samples was observed by SEM and EDS. The dried pellets previously immersed in SBF for 3, 7, and 14 days were analyzed by X-ray diffraction using glancing incidence geometry. The diffractometer model Philips X'Pert MRD (Cu Kα radiation = 1.5418 Å) was configured with a parallel mirror in the incident beam and a parallel plate collimator in the diffracted beam path to allow a constant low-angle incidence (1°) glancing the sample surface. The X-ray measurements were taken at 45 kV, 40 mA in a 3−50° 2θ range, with 0.05° step size and 0.3°/min speed. The concentrations of Ca and P in the supernatant fluid were determined by inductively coupled plasma (ICP) (Jobin−Yvon JY70 Plus spectrometer), and the pH measured with a standard pH electrode.

Cell Culture and in Vitro Assays. The MG63 osteosarcoma cell line was routinely maintained in DMEM/F12 growth medium (PAA, Pasching, Austria) supplemented with 10% heat inactivated FBS (PAA) and buffered with Hepes (Sigma, Sain Louis, MO). The medium was changed every day. The survival/toxicity assays were carried out with 1000 MG63 cells well seeded in 96-well plates. Cells were allowed to attach for 24 h prior to **CaP1** treatment. **CaP1** was mixed with DMEM/F12 medium buffered with Hepes +10% FBS to a stock concentration of 35 mg/mL. The solution was incubated for 24 h at 37 °C. Since not all **CaP1** dissolved, the supernatant (with equivalent of 12 mg/mL **CaP1**) was recovered and used to treat the cells. The treatment was carried out for 6 days, with medium changes every 24 h. At the time of the medium change, the cell metabolic activity was measured using the Presto Blue resazurin-based reagent, according to the manufacturer's protocol (Life Technologies). Two independent experiments were carried out in quadruplicate. Statistical differences were evaluated with One-Way ANOVA and Dunnnet's post test. The effect of **CaP1** on cell numbers was evaluated by counting cells. For this purpose, cells were seeded in 24-well plates (5000 cells/well) in growth medium buffered with Hepes and allowed to attach for 24 h. Next, they were treated with different concentrations of **CaP1** (prepared as described above) for 6 days, with medium changes every other day. Cells were detached, stained with trypan blue and counted in a TC-20 automatic counter (BioRad).

DOI: 10.1021/acs.inorgchem.5b01634
Inorg. Chem. 2015, 54, 9929−9935

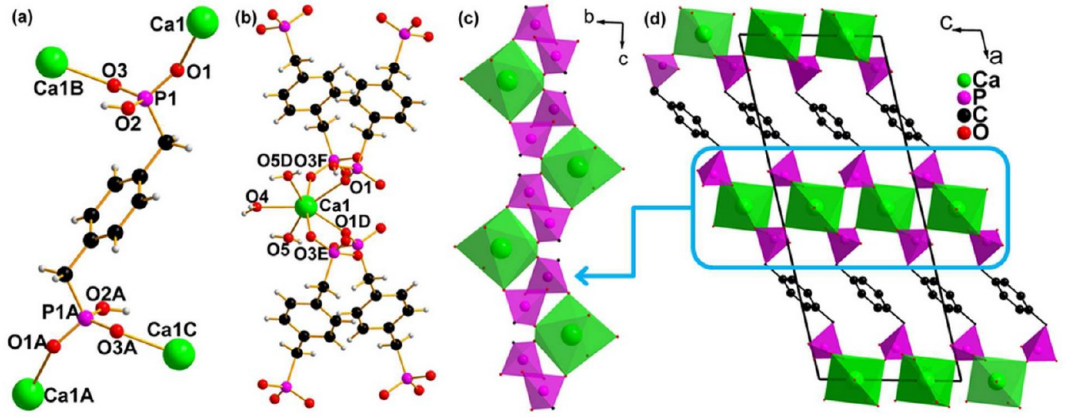

Figure 1. Structural features of **CaP1**: (a) coordination mode of PXBP ligand; (b) coordination environment of Ca^{2+}. (c) Ca^{2+} ions are interconnected via double phosphonate groups forming an infinite inorganic chain, which was converted from the inorganic layer circled in (d). (d) Unit cell of **CaP1** viewed along *b* axis. Symmetry codes: A, 1.5−*x*, 1.5−*y*, 1−*z*; B, 2−*x*, 1−*y*, 1−*z*; C, −0.5+*x*, 0.5+*y*, *z*; D, 2−*x*, *y*, 0.5−*z*; E, 2−*x*, 1−*y*, 1−*z*; F, *x*, 1−*y*, −0.5+*z*.

The experiment was repeated twice and carried out in quadruplicate. Statistical differences were evaluated with One-Way ANOVA and Dunnnet's post test. Finally, calcification was evaluated on MG63 cells cultured in 96-well plates grown in DMEM/F12 medium +10% FBS + **CaP1** in the indicated concentrations. The medium was changed every other day and cells kept for a period of 4 weeks. Then, cells were fixed in 10% formalin for 10 min, washed with PBS stained with 2% alizarin red S, pH 4.2 (Sigma) for 5 min, washed, and observed with a Nikon TiU inverted microscope. Images were taken with NiS software and the same corrections were applied to all photographs.

RNA Extraction and Quantitative Real-Time PCR (qPCR). Total RNA was extracted from MG63 cells using Trizol Reagent (Invitrogen, Carlsbad, CA, USA) and genomic DNA present in the samples was eliminated using TURBO DNA-free (Ambion, Applied Biosystems, Foster City, CA, USA), following the manufacturer's instructions. cDNA synthesis was performed using the NZY First-strand cDNA Synthesis Kit (NZY Tech). Runx2 and Spp1 transcripts were quantified by real-time quantitative PCR (qPCR) using ready-made primers and SYBR Green (BioRad). The expression assays were performed in 96-well plates in a CFX connect real-time PCR system (BioRad). The quantification method used was from a standard curve. All samples were analyzed in triplicate, and the mean C_t value used for data analysis.

RESULTS AND DISCUSSION

General Aspects. The two new Ca-bearing Metal Organic Frameworks were synthesized under similar conditions (excess of Ca^{2+}, hydrothermal method, 180 °C, for 3 days) using two different pH values. **CaP1** is obtained in strong acidic conditions (pH ≤ 2), while at pH ≥ 3 **CaP2** crystallizes as a pure phase containing a very small amount of $Ca(OH)_2$ (Figure S2). SEM image of **CaP1** (Figure S3, left) shows uniform prisms, while **CaP2** (Figure S3) consists of very thin plates. TGA plot of **CaP1** from 40 to 215 °C shows three weight-loss stages corresponding to the release of three coordinate water molecules (Figure S4 and Experimental Section), whereas for **CaP2**, the water molecules are removed completely only at ca. 280 °C. In **CaP1**, Ca−H_2O bond lengths are different (d_{Ca-O4} = 2.4350 Å, d_{Ca-O5} = 2.4148 Å. Table S2) and the hydrogen-bonding interactions involving O4 as donor are clearly weaker than those of O5 (Table S3). These facts explain why O4 water molecules are lost at a temperature lower than O5. For similar reasons, the **CaP2**-bonded water molecules (O10 and O11, Tables S2 and S3) are lost at different temperatures. Moreover, the extensive network of hydrogen-bonding interactions helps stabilizing the coordinated water molecules (Figures S8, S9).

Structure Description. **CaP1** crystallizes in the monoclinic *C*2/*c* space group (Table S1), with the asymmetric unit (Figure S5) containing a single independent calcium atom (Ca1). The PXBP ligand coordinates to four Ca atoms (Figure 1a). The sevenfold Ca atoms are coordinated by four O atoms from four symmetry-related PXBP ligands and three water molecules (Figure 1b). Even though all water molecules act as terminal ligands the phosphonate ligands act as pillars linking neighboring Ca atoms (Figure 1d) forming a three-dimensional framework containing one-dimensional inorganic chains (Figure 1c and Figure 1d).

CaP2 crystallizes in the triclinic $P\bar{1}$ space group (Table S1), with the asymmetric unit containing two independent calcium atoms (Ca1 and Ca2, Figure S6). The PXBP ligand shows two kinds of different coordination modes to Ca atoms (Figure 2a). The sevenfold Ca1 is coordinated by six O atoms from five PXBP ligands and one water molecule while the sixfold Ca2 is

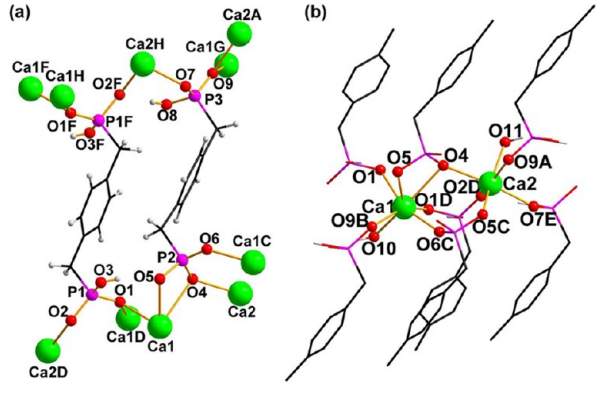

Figure 2. (a) Coordination modes of the PXBP ligand in **CaP2**; (b) coordination environments of 7-coordinated Ca1 and 6-coordinated Ca2. For clarity, the end phosphonate groups and some hydrogen atoms were omitted and all atoms are drawn as wires, except for coordinate oxygen and calcium atoms that are depicted as ball and sticks. Symmetry codes: A, 1−*x*, −*y*, −*z*; B, *x*, 1+*y*, 1+*z*; C, 1−*x*, 1−*y*, 1−*z*; D, −*x*, 1−*y*, 1−*z*; E, *x*, *y*, 1+*z*; F, −*x*, 1−*y*, −*z*; G, *x*, −1+*y*, −1+*z*; H, *x*, *y*, −1+*z*.

DOI: 10.1021/acs.inorgchem.5b01634
Inorg. Chem. 2015, 54, 9929−9935

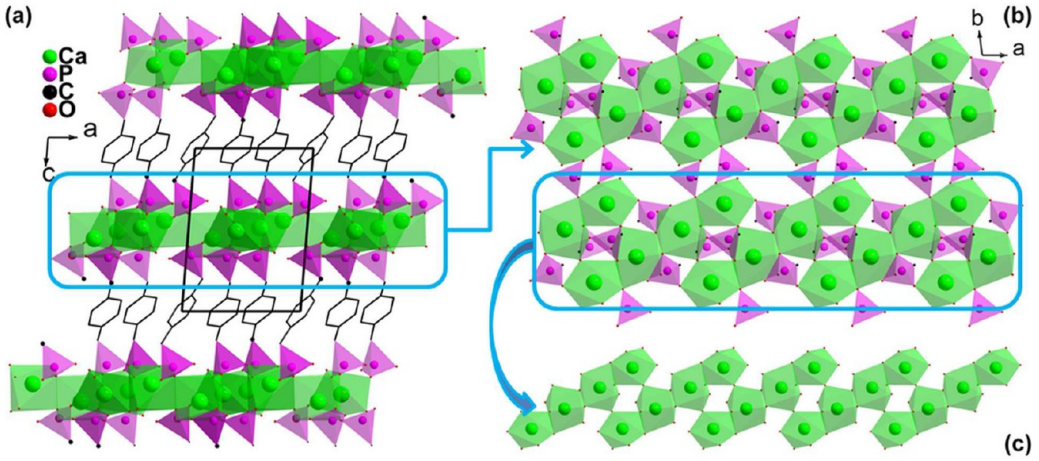

Figure 3. (a) Unit cell of **CaP2** viewed along the *b* axis (hydrogen atoms were omitted for clarity); (b) inorganic layer viewed along the *c* axis (hydrogen and carbon atoms were omitted for clarity); (c) infinite inorganic ribbon of calcium oxide obtained by omission of the phosphorus atoms.

coordinated by five O atoms from five PXBP ligands and also one water molecule (Figure 2b and Figure S7).

CaP2 is also a three-dimensional framework (Figure 3a) comprising pillaring ligands linking inorganic layers (Figure 3b) hosting ribbons (Figure 3c) of Ca atoms connected via phosphonate groups. The ribbons consist of four edge-sharing Ca atoms (two Ca1 at the center and two external Ca2) linked via corner-sharing O4 atoms, which is reminiscent of other inorganic subnetworks.[21,22] The closest Ca1—Ca1 distance is 3.7415(8) Å and Ca1—Ca2 = 3.6570(9) Å (Table S2).

The Ca−H_2O bond distances in **CaP1** spun from 2.4148(16) (d_{Ca1-O5}) to 2.435(2) Å (d_{Ca1-O4}, Table S2) clearly larger than those in **CaP2**, 2.365(2) ($d_{Ca2-O11}$) and 2.386(2) Å ($d_{Ca2-O10}$), indicating that the removal of water molecules is easier for **CaP1**. This conclusion is consistent with TG data (Experimental Section, Figure S4).

Tests with SBF. After immersion of pressed pellets of **CaP1** and **CaP2** in Kokubos's SBF for 3, 7, 9, 12, and 14 days, the surface of the pellets was observed by SEM/EDS and the supernatant fluid analyzed by ICP. No calcium-phosphate precipitation on the surface of the **CaP2** pellets or change in the Ca/P molar ratio of the supernatant liquids (even after 14 days of soaking) was observed and, thus, **CaP2** is inert in SBF solution. In contrast, in the same conditions, a layer of precipitated calcium phosphate was seen on the surface of the **CaP1** pellets (Figure 4 and Figure 5), whose Ca/P molar ratio was determined by EDS (Ca/P_{EDS}) (Table 1). After 3 days of soaking in SBF, the pH of the solution dropped from 7.4 to 6.8 and a layer of lamellar calcium phosphate formed, with a Ca/P molar ratio of ca. 1.3 (Figure 4) close to that of octacalcium phosphate (OCP, $Ca_8H_2(PO_4)_6{\cdot}5H_2O$), 1.33. After 7 days in SBF, the Ca/P ratio increased to ca. 1.8, closer to 1.67, the value for hydroxyapatite, $Ca_{10}(PO_4)_6(OH)_2$ (HAP), and concomitantly the pH of the supernatant liquid decreased to 6.4. According to Johnsson and Nancollas[23] OCP may form in this pH range as a precursor for hydroxyapatite.[24]

The precipitates formed on the surface of pellets immersed in SBF for 3, 7, and 14 days were studied by grazing incidence X-ray diffraction (Figure 6). Clearly, upon increasing the soaking time the **CaP1** reflections become weaker while the intensity of peaks from, at least, two phases, most likely OCP and hydroxyapatite, increases.

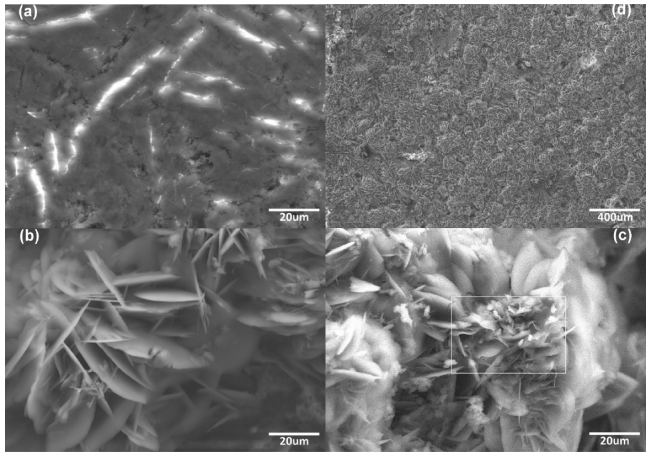

Figure 4. SEM images of **CaP1** pellet surface: (a) prior to soaking in SBF; (b) after soaking in SBF for 3 days, exhibiting a film of lamellar calcium phosphate crystals; (c) side view of a pellet after soaking in SBF for 3 days at high magnification, the middle square indicates where the EDS spectrum was acquired; (d) overall pellet surface of **CaP1** showing a film of lamellar calcium phosphate crystals.

Although the straightforward SBF test clearly suggests that **CaP1** is able to promote the formation of bone-precursor phases it presents several limitations as a technique to evaluate the material's bioactive potential.[25,26] Therefore, the bioactivity of **CaP1** was next assessed using the osteoblast-like MG63 cell line.

Cytotoxicity Tests. The effect of **CaP1** on the MG63 cell viability was analyzed using a standard survival/toxicity test based on the reduction of resazurin by mitochondrial reductase. Thus, an increase of the reduced product (absorbing at 570 nm) vs the oxidized substrate given to the cells (absorbing at 600 nm) indicates healthy and viable cells, a measure which in most cases may be directly translated to an increase in cell number. The MG63 cells looked healthy and continued to proliferate during the whole incubation period. A slight reduction in the amount of product reduced was observed for higher concentrations of **CaP1** (2−6 mg/mL; $p < 0.05$), after 6 days incubation (Figure 7a). This result was confirmed by counting cells, and these concentrations of **CaP1** also significantly reduced cell number (Figure 7b).

DOI: 10.1021/acs.inorgchem.5b01634
Inorg. Chem. 2015, 54, 9929−9935

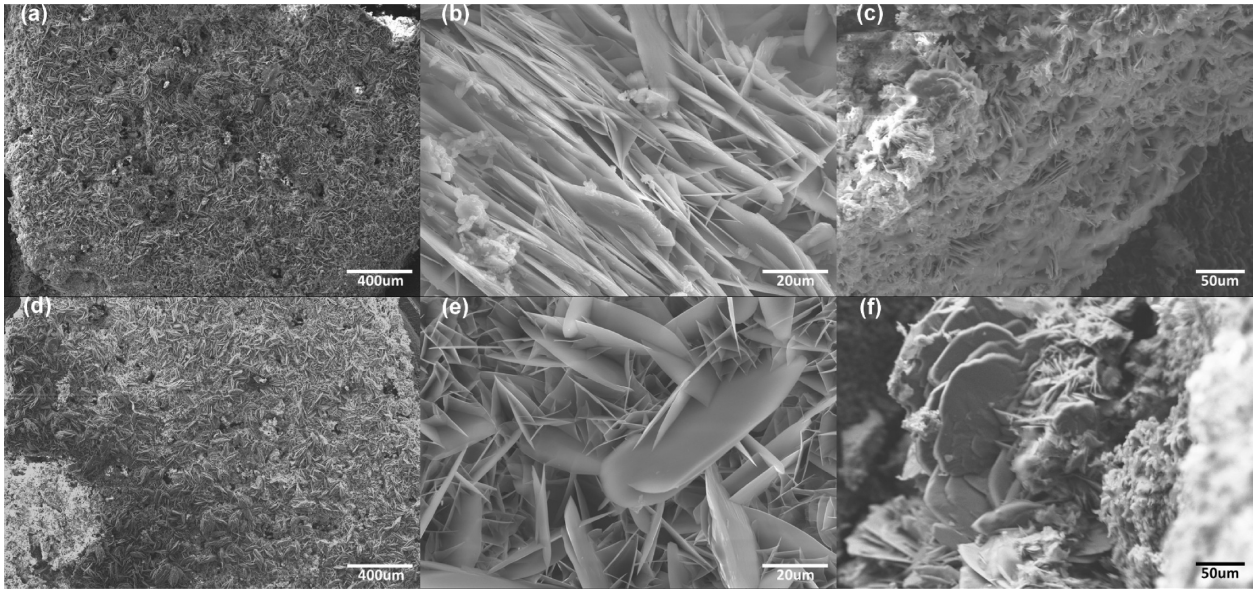

Figure 5. SEM images of **CaP1** pellet surface after soaking in SBF for 7 (Top) and 14 (Bottom) days exhibiting a clear surface modification with lamellar calcium phosphate crystals: (a) overview of the pellet surface; (b) high magnification showing lamellar crystal particles on the surface; (c) side view of the pellet; (d) overview of the pellet surface; (e) high magnification showing lamellar crystal particles on the surface; (f) side view of the pellet.

Table 1. Ca/P Molar Ratio of Both Calcium Phosphate Phases Precipitated at the Surface of CaP1 Pellets (Ca/P_{EDS}) and Supernatant Liquids (Ca/P_{ICP}), and pH of Supernatant Liquids, Obtained Following Immersion in SBF

days in SBF	Ca_{ICP} mg·L^{-1} (±1)	P_{ICP} mg·L^{-1} (±1)	pH (±0.1)	Ca_{EDS} at·% (±0.7)	P_{EDS} at·% (±0.5)	Ca/P_{EDS}
0	97	33	7.4	42.7	57.3	0.7
3	158	254	6.8	56.8	43.2	1.3
7	151	283	6.4	64.3	35.7	1.8
9	143	274	6.4	63.2	36.8	1.7
12	141	273	6.4	62.1	37.9	1.6
14	141	270	6.4	60.6	39.4	1.5

Cell morphology observed with phase contrast microscopy did not show any alterations in **CaP1** treated cells, relative to the untreated control (Figure 8). Alizarin, which stains extracellular calcium deposits, disclosed a dose-dependent calcification in cells treated with 6 and 3 mg/mL **CaP1** relatively to the untreated control. Thus, **CaP1** seems to promote *in vitro* bone-like mineralization.

CaP1 concentrations of 6−2 mg/mL significantly reduced the cell number, in agreement with the observed increase in calcification. This is because as cells differentiate they reduce their proliferation rate, yet another indication of the bioactivity of **CaP1**.

Following 2 weeks treatment with **CaP1**, mRNA levels of Runx2, which is the master regulator of osteoblastogenesis and directs transcriptional programs essential for bone formation, and its downstream regulated gene Spp1 (osteopontin/secreted phosphoprotein 1) were measured by qPCR. mRNA from both genes increased with **CaP1** treatment (Figure 9). In summary, **CaP1** induces successful *in vitro* bone formation. **CaP1** in concentrations of 6−2 mg/mL significantly reduced cell number in agreement with differentiation characterized by induction of Runx2 and Spp1, which in turn arrests the cells in G1/S checkpoint,[27] promoting mineralization as observed by the increase in calcification.

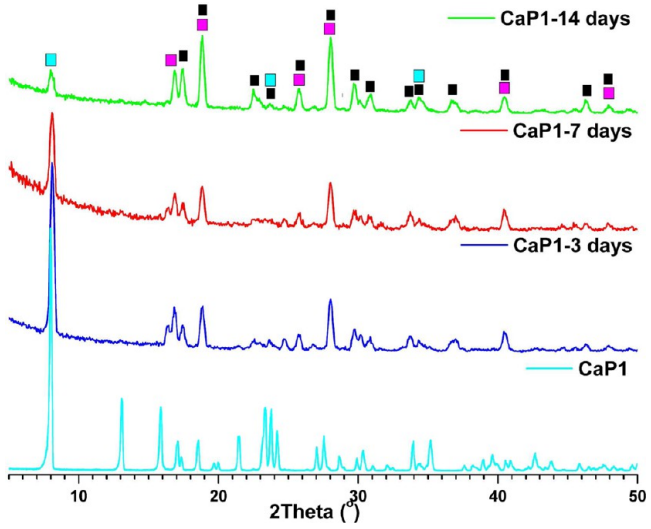

Figure 6. Powder X-ray diffraction pattern of **CaP1** and grazing incidence X-ray diffraction patterns of the **CaP1** calcium phosphate surface precipitates formed after immersion in SBF for 3, 7, and 14 days. The squares depict a tentative assignment of reflections to **CaP1** (light blue), OCP (black), and hydroxyapatite (pink).

CONCLUSIONS

In conclusion, dense three-dimensional $[Ca(H_2O)_3(HPXBP)]$ (**CaP1**) and $[Ca_2(H_2O)_2(HPXBP)_{1.5}]$ (**CaP2**) (PXBP: *p*-xylylenebisphosphonate) add to the very short list of Ca-bearing Metal Organic Frameworks. While **CaP2** is essentially bioinert, in the context of osteogenesis, **CaP1** readily precipitates bone-precursor phases (calcium phosphates OCP and hydroxyapatite) in synthetic human blood plasma. Moreover, studies with MG63 cells indicate that **CaP1** is not toxic and stimulates bone-like mineralization. The present

DOI: 10.1021/acs.inorgchem.5b01634
Inorg. Chem. 2015, 54, 9929−9935

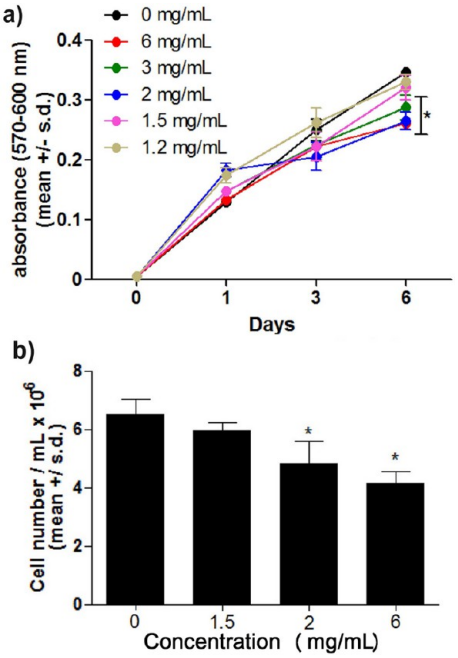

Figure 7. Evaluation of **CaP1** toxicity in MG63 osteoblast-like cells grown in DMEM/F12 medium buffered with Hepes + 10% FBS for the indicated time points with or without varying concentrations of **CaP1**. The medium was changed every other day. (a) Cell viability measured as rezasurin (600 nm) reduction (570 nm) by the mitochondria during the aerobic respiration of the cells. (b) Cell number after 6 days incubation. *: $p < 0.05$, One-Way ANOVA, Dunnet's post test.

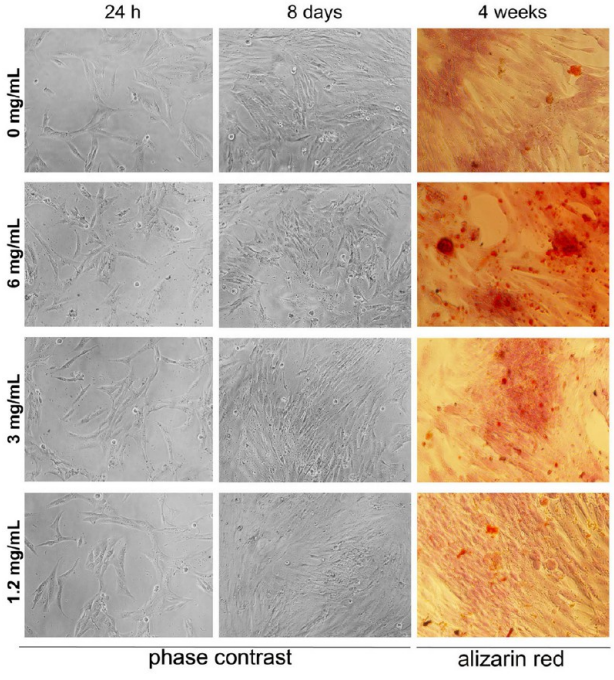

Figure 8. MG63 cells grown in DMEM/F12 medium buffered with HEPES + 10% FBS with or without **CaP1**. Following 4 weeks incubation (medium changed every other day) the cells were fixed in 10% formalin for 10 min and stained with alizarin red. Phase contrast, 10× magnification; bright field, 20× magnification.

compounds, particularly **CaP1**, hold potential for treating bone disorders, such as osteoporosis.

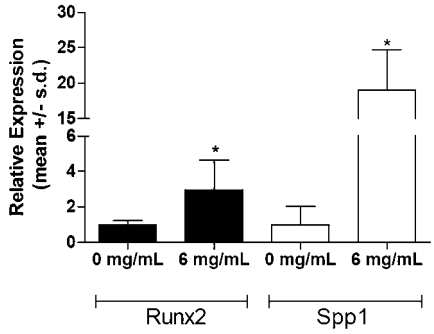

Figure 9. Differentiation of MG63 osteoblast-like cells. Cells were treated with **CaP1** for 15 days and Runx2 and Spp1 mRNA levels were evaluated by qPCR. *: $p < 0.05$ vs control; Student's t test.

■ ASSOCIATED CONTENT

Supporting Information

The Supporting Information is available free of charge on the ACS Publications website at DOI: 10.1021/acs.inorgchem.5b01634.

Crystallographic data (CIF)
Check CIF (PDF)
Single crystal data, bond lengths and angles and hydrogen bonding information on **CP1** and **CP2** in Table S1−Table S3, Powder PXRD patterns of **CP1** and **CP2**SEM images, TGA plots, asymmetric units and coordination spheres of Ca metal (PDF)
Crystallographic data (CIF)
Check CIF (PDF)

■ AUTHOR INFORMATION

Corresponding Author

*E-mail: rocha@ua.pt.

Notes

The authors declare no competing financial interest.

■ ACKNOWLEDGMENTS

This work was developed in the scope of the project CICECO-Aveiro Institute of Materials (ref. FCT UID/CTM/50011/2013), financed by national funds through the FCT/MEC and when applicable cofinanced by FEDER under the PT2020 Partnership Agreement. We acknowledge projects CENTRO-07-ST24-FEDER-002030, MI-PI-36-ARH/2012, MI-PI-08-ARH/2014, PTDC/CTM-NAN/119994/2010 and grant PTDC/SAU-ONC/118346/2010 (LAH). Dr. Rosário Soares help in the grazing incidence XRD measurements is acknowledged.

■ REFERENCES

(1) Weaver, C. M. *Curr. Osteoporos. Rep.* **2014**, *12*, 211−8.
(2) Pereira, P. C. *Nutrition* **2014**, *30* (6), 619−27.
(3) Zhu, K.; Prince, R. L. *Clin. Biochem.* **2012**, *45*, 936−42.
(4) Rizzoli, R. *Best Pract. Res., Clin. Endocrinol. Metab.* **2008**, *22* (5), 813−29.
(5) Hitz, M. F.; Eskildsen, P. C.; Jensen, J. B. *Calcif. Tissue Int.* **2005**, *77*, 361−6.
(6) Cline, J. *Topics Compan. Animal Med.* **2012**, *27*, 159−64.
(7) Drake, M. T.; Clarke, B. L.; Khosla, S. *Mayo Clin. Proc.* **2008**, *83* (9), 1032−45.
(8) Major, P. P.; Lipton, A.; Berenson, J.; Hortobagyi, G. *Cancer* **2000**, *88*, 6−14.

DOI: 10.1021/acs.inorgchem.5b01634
Inorg. Chem. 2015, 54, 9929−9935

(9) *WebCSD* v 1.1.1; Cambridge Structural Database; Database last updated: February 18, 2015.
(10) Bishop, M.; Bott, S. G.; Barron, A. R. *Chem. Mater.* **2003**, *15*, 3074−88.
(11) Stock, N.; Stoll, A.; Bein, T. *Microporous Mesoporous Mater.* **2004**, *69*, 65−69.
(12) Colodrero, R. M. P.; Cabeza, A.; Olivera-Pastor, P.; Papadaki, M.; Rius, J.; Choquesillo-Lazarte, D.; García-Ruiz, J. M.; Demadis, K. D.; Aranda, M. A. G. *Cryst. Growth Des.* **2011**, *11*, 1713−22.
(13) Liang, X.; Zhang, F.; Feng, W.; Zou, X.; Zhao, C.; Na, H.; Liu, C.; Sun, F.; Zhu, G. *Chem. Sci.* **2013**, *4*, 983−92.
(14) Bazaga-García, M.; Colodrero, R. M. P.; Papadaki, M.; Garczarek, P.; Zoń, J.; Olivera-Pastor, P.; Losilla, E. R.; León-Reina, L.; Aranda, M. A. G.; Choquesillo-Lazarte, D.; Demadis, K. D.; Cabeza, A. *J. Am. Chem. Soc.* **2014**, *136*, 5731−9.
(15) Liu, D.; Kramer, S. A.; Huxford-Phillips, R. C.; Wang, S.; della Rocca, J. D.; Lin, W. *Chem. Commun.* **2012**, *48*, 2668−70.
(16) Alvarez, E.; Marquez, A. G.; Devic, T.; Steunou, N.; Serre, C.; Bonhomme, C.; Gervais, C.; Izquierdo-Barba, I.; Vallet-Regi, M.; Laurencin, D.; Maurif, F.; Horcajada, P. *CrystEngComm* **2013**, *15*, 9899−05.
(17) Sheldrick, G. M. *SHELXS-97, Program for Crystal Structure Solution*; University of Göttingen, 1997.
(18) Sheldrick, G. M. *SHELXL-97, Program for Crystal Structure Refinement*; University of Göttingen, 1997.
(19) Spek, A. L. *Acta Crystallogr., Sect. D: Biol. Crystallogr.* **2009**, *D65*, 148−155.
(20) Kokubo, T.; Takadama, H. *Biomaterials* **2006**, *27*, 2907−15.
(21) Shi, F. − N.; Silva, A. R.; Bian, L. *J. Solid State Chem.* **2015**, *225*, 45−52.
(22) Yang, T.; Ferreira, R. A. S.; Carlos, L. D.; Rocha, J.; Shi, F.-N. *RSC Adv.* **2014**, *4*, 7818−25.
(23) Johnsson, M. S.; Nancollas, G. H. *Crit. Rev. Oral Biol. Med.* **1992**, *3*, 61−82.
(24) Ito, N.; Kamitakahara, M.; Yoshimura, M.; Ioku, K. *Mater. Sci. Eng., C* **2014**, *40*, 121−6.
(25) Bohner, M.; Lemaitre, J. *Biomaterials* **2009**, *30*, 2175−9.
(26) Pan, H. B.; Zhao, X. L.; Darvell, B. W.; Lu, W. W. *Acta Biomater.* **2010**, *6*, 4181−8.
(27) Thomas, D. M.; Johnson, S. A.; Sims, N. A.; Trivett, M. K.; Slavin, J. L.; Rubin, B. P.; Waring, P.; McArthur, G. A.; Walkley, C. R.; Holloway, A. J.; Diyagama, D.; Grim, J. E.; Clurman, B. E.; Bowtell, D. D.; Lee, J. S.; Gutierrez, G. M.; Piscopo, D. M.; Carty, S. A.; Hinds, P. W. *J. Cell Biol.* **2004**, *167* (5), 925−34.

DOI: 10.1021/acs.inorgchem.5b01634
Inorg. Chem. 2015, 54, 9929−9935